# Organoplatinum Dendrimers

Sudhir Achar, Jagadese J. Vittal, and Richard J. Puddephatt*

*Department of Chemistry, University of Western Ontario, London, Canada N6A 5B7*

*Received June 1, 1995*[⊗]

A route to dendrimeric organoplatinum complexes is described by a strategy involving oxidative addition of the C−Br bonds of 4,4′-$(BrCH_2)_2$-2,2′-$(C_5H_3N)_2$, **A**, to $[PtMe_2(bu_2bipy)]$, **1**, $bu_2bipy$ = 4,4′-di-*tert*-butyl-2,2′-bipyridine, to give 4,4′-$\{BrPtMe_2(bu_2bipy)CH_2\}_2$-2,2′-$(C_5H_3N)_2$, **2**, followed by regeneration of a $[PtMe_2(NN)]$ functionality by reaction of the free diimine group of **2** with $[Pt_2Me_4(\mu\text{-}SMe_2)_2]$, **B**, to give 4,4′-$\{BrPtMe_2(bu_2bipy)CH_2\}_2$-2,2′-$(C_5H_3N)_2PtMe_2$, **3**. Repetition of this cycle has given dendrimers containing 6, 7, and 14 platinum atoms. The structure of **3** has been determined crystallographically. The above complexes containing 1, 3, or 7 platinum atoms react with the tetrafunctional core 1,2,4,5-$(BrCH_2)_4C_6H_2$ in a 4:1 ratio by oxidative addition of the C−Br bonds to the platinum(II) center to give dendrimers containing 4, 12, or 28 platinum atoms, respectively. An oligomeric dendrimer is prepared by reaction of **A** with **B**.



## Introduction

There is much current interest in the synthesis and properties of molecular dendrimers.[1] Most such compounds are organic,[2] but routes to dendrimers containing silicon,[3] phosphorus,[4] or transition metals[5,6] have also been developed recently. The synthesis of dendrimeric coordination compounds is usually based on ligand substitution with multifunctional ligands and often involves the need for protection/deprotection sequences.[5] Most organotransition metal dendrimers have the metal either at the core only or at the periphery only, with the remainder based on organic chemistry. One major problem in devising routes to organometallic dendrimers with metals in each layer is that individual steps do not occur in sufficiently high yield to provide pure complexes directly and that separation procedures using chromatography are often not applicable. Since dendrimers must be built up layer-by-layer, usually with isolation and purification at each step, very high yields are imperative in every individual step if a multistep synthesis is to be accomplished without chromatographic purification steps. It has been shown that oxidative addition of primary alkyl or benzyl halides, RX, to $[PtMe_2(NN)]$ gives $[PtXMe_2R(NN)]$, NN = diimine ligand such as 2,2′-bipyridine,[7] and that $[PtMe_2(NN)$ can be prepared from $[Pt_2Me_4(\mu\text{-}SMe_2)_2]$ and the ligand NN,[8] both in essentially quantitative yields (eqs 1 and 2). A strategy was then devised to

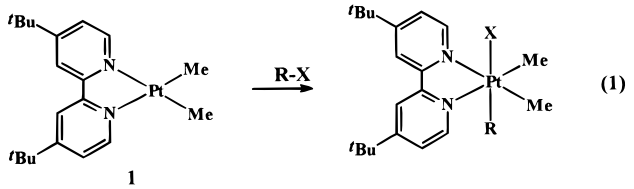


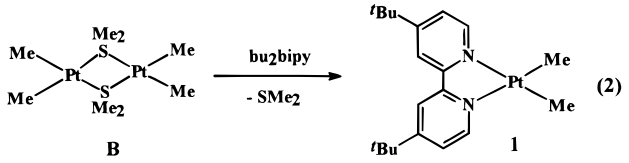


prepare organoplatinum dendrimers by using a reagent containing *both* alkyl halide and diimine functionalities, and the resulting chemistry forms the basis of this paper. Preliminary accounts of the research[9] and of related chemistry[10] have been published.

## Results and Discussion

**First Synthetic Cycle.** One key reagent in this work is 4,4′-bis(bromomethyl)-2,2′-bipyridine, **A**, which

[⊗] Abstract published in *Advance ACS Abstracts,* November 15, 1995.

(1) (a) Issberner, J.; Moors, R.; Vogtle, F. *Angew. Chem., Int. Ed. Engl.* **1995**, *33*, 2413. (b) Mekelburger, H. B.; Jaworek, W.; Vogtle, F. *Angew. Chem., Int. Ed. Engl.* **1992**, *31*, 1571.

(2) (a) Xu, Z. F.; Kahr, M.; Walker, K. L.; Wilkins, C. L.; Moore, J. S. *J. Am. Chem. Soc.* **1994**, *116*, 4537. (b) Jansen, J. F. G. A.; Debrabandervandenberg, E. M. M.; Meijer, E. W. *Science* **1994**, *266*, 1226.

(3) (a) Vandermade, A. W.; Vanleeuwen, P. W. N. M.; Dewilde, J. C.; Brandes, R. A. C. *Adv. Mater.* **1993**, *5*, 466. (b) Seyferth, D.; Son, D. Y.; Rheingold, A. L.; Ostrander, R. L. *Organometallics* **1994**, *13*, 2682. (c) Alonso, B.; Cuadrado, I.; Moran, M.; Losada, J. *J. Chem. Soc., Chem. Commun.* **1994**, 2575. (d) Lambert, J. B.; Pflug, J. L.; Stern, C. L. *Angew. Chem., Int. Ed. Engl.* **1995**, *34*, 98. (e) Knapen, J. W. J.; Van der Made, A. W.; De Wilde, J. C.; Van Leeuwen, P. W. N. M.; Wijkens, P.; Grove, D. M.; Van Koten, G. *Nature* **1994**, *372*, 659.

(4) (a) Launay, N.; Caminade, A. M.; Lahana, R.; Majoral, J. P. *Angew. Chem., Int. Ed. Engl.* **1994**, *33*, 1589. (b) Launay, N.; Caminade, A. M.; Majoral, J. P. *J. Am. Chem. Soc.* **1995**, *117*, 3282. (c) Miedener, A.; Curtis, C. J.; Barkley, R. M.; Dubois, D. L. *Inorg. Chem.* **1994**, *33*, 5482. (d) Brunner, H.; Bublak, P. *Synthesis* **1995**, 36.

(5) (a) Balzani, V.; Campagna, S.; Denti, G.; Juris, A.; Serroni, S.; Venturi, M. *Coord. Chem. Rev.* **1994**, *132*, 1. (b) Serroni, S.; Denti, G.; Campagna, S.; Juris, A.; Ciano, M.; Balzani, V. *Angew. Chem., Int. Ed. Engl.* **1992**, *31*, 1493. (c) Campagna, S.; Giannetto, A.; Serroni, S.; Denti, G.; Trusso, S.; Mallamace, F.; Micali, N. *J. Am. Chem. Soc.* **1995**, *117*, 1754. (d) Newcome, G. R.; Cardullo, F.; Constable, E. C.; Moorefield, C. N.; Thompson, A. M. W. C. *J. Chem. Soc., Chem. Commun.* **1993**, 925. (e) Turro, C.; Niu, S. F.; Bossmann, S. H.; Tomalia, D. A.; Turro, N. J. *J. Phys. Chem.* **1995**, *99*, 5512.

(6) (a) Liao, Y.-H.; Moss, J. R. *Organometallics* **1995**, *14*, 2130. (b) Liao, Y.-H.; Moss, J. R. *J. Chem. Soc., Chem. Commun.* **1993**, 1774. (c) Mouline, F.; Gloaguen, B.; Astruc, D. *Angew. Chem., Int. Ed. Engl.* **1992**, *31*, 458.

(7) (a) Ferguson, G.; Parvez, M.; Monaghan, P. K.; Puddephatt, R. J. *J. Chem. Soc., Chem. Commun.* **1983**, 267. (b) Monaghan, P. K.; Puddephatt, R. J. *Organometallics* **1984**, *3*, 444. (c) Monaghan, P. K.; Puddephatt, R. J. *Organometallics* **1985**, *4*, 1405. (d) Scott, J. D.; Puddephatt, R. J. *Organometallics* **1986**, *5*, 1538. (e) Crespo, M.; Puddephatt, R. J. *Organometallics* **1987**, *6*, 2548. (f) Monaghan, P. K.; Puddephatt, R. J. *J. Chem. Soc., Dalton. Trans.* **1988**, 595. (g) Aye, K. T.; Canty, A. J.; Crespo, M.; Puddephatt, R. J.; Scott, J. D.; Watson, A. A. *Organometallics* **1989**, *8*, 1518.

(8) Scott, J. D.; Puddephatt, R. J. *Organometallics* **1983**, *2*, 1643.

(9) (a) Achar, S.; Puddephatt, R. J. *Angew. Chem., Int. Ed. Engl.* **1994**, *33*, 847. (b) Achar, S.; Puddephatt, R. J. *J. Chem. Soc., Chem. Commun.* **1994**, 1895.

(10) Achar, S.; Puddephatt, R. J. *Organometallics* **1995**, *14*, 1681.

0276-7333/96/2315-0043$12.00/0 

**Scheme 1**

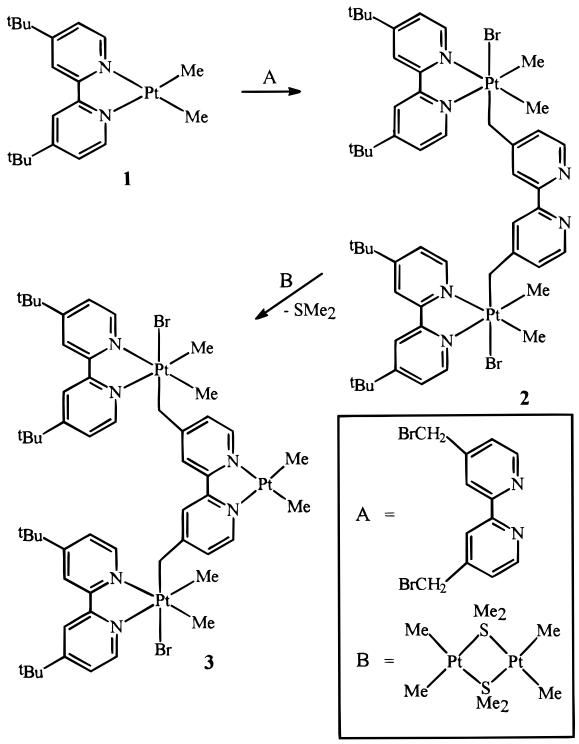


is synthesized by the bromination of 4,4′-dimethyl-2,2′-bipyridine with *N*-bromosuccinimide.[11] This compound **A** reacts with [$PtMe_2$($bu_2$bipy)], **1**, $bu_2$bipy = 4,4′-di-*tert*-butyl-2,2′-bipyridine, according to Scheme 1 to give the diplatinum(IV) complex **2** in essentially quantitative yield. The ligand $bu_2$bipy is used in this chemistry instead of the simpler 2,2′-bipyridine because it enhances the solubility of the products.[12] The *tert*-butyl groups are sufficiently removed from the platinum center in **1** that they do not cause steric hindrance to oxidative addition. As in oxidative additions to [$PtMe_2$-(2,2′-bipyridine)],[7] the reaction occurs with a color change from the characteristic orange-red color of **1** to a very pale yellow color of **2**. The color of the platinum(II) complex arises due to the presence of a platinum(II) 5d−diimine($\pi^*$) metal-to-ligand charge transfer band (MLCT) band in the visible region of the spectrum[7] which moves to the UV region in the platinum(IV) product **2** (Figure 1). The $^1$H NMR spectrum of **2** contained a single resonance for the $Me_2Pt$ groups, and the magnitude of $^2J$(PtH) decreased from 86 Hz in **1** to 69 Hz in **2**, typical of the difference between platinum(II) and platinum(IV) methyl complexes.[7] The $CH_2Pt$ resonance was observed at $\delta = 2.73$ with $^2J$(PtH) = 98 Hz, and the *t*-Bu protons appeared as a singlet at $\delta =$ 1.13. The coupling $^3J$(PtH) to the ortho protons of the $bu_2$bipy ligand decreased from 22 Hz in **1** to 18 Hz in **2**. Note that the product **2** is clearly that of *trans* oxidative addition: the alternative product of *cis* oxidative addition should give two MePt, *t*-Bu, and $CH_2Pt$ resonances.[7] The FAB mass spectrum of **2** contained a molecular ion peak at $m/z = 1329$, with the expected isotope pattern.

Complex **2** contains a free bipyridyl functionality, and so it can act as a ligand. Thus **2** reacted with [$Pt_2Me_4$-

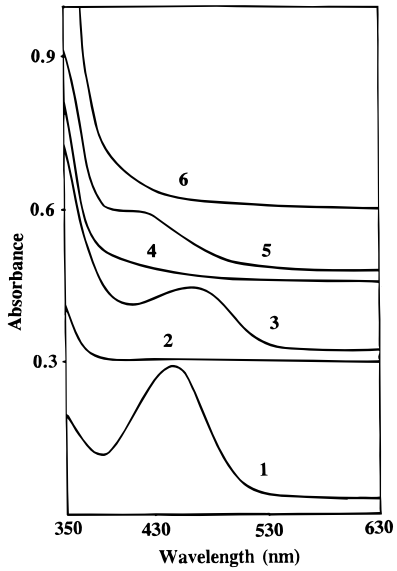


**Figure 1.** UV−visible spectra of selected complexes. Note the MLCT band in the 400−500 nm region for **1**, **3**, and **5** but not for **2**, **4**, and **6**. Spectra are offset for clarity.

($\mu$-$SMe_2)_2$], **B**, with displacement of the $\mu$-$SMe_2$ ligands, to give the triplatinum complex **3** (Scheme 1). The UV−visible spectrum of complex **3** contains a metal-to-ligand charge transfer band [platinum(II) 5d to diimine($\pi^*$)] with $\lambda_{max} = 474$ nm (Figure 1), and hence **3** is orange-red in color.[7,13] The $^1$H NMR spectrum of **3** exhibits two methyl−platinum resonances in a 1:2 ratio, which are assigned to the $Me_2Pt^{II}$ {$\delta = 0.77$, $^2J$(PtH) = 86 Hz} and $Me_2Pt^{IV}$ {$\delta = 1.50$, $^2J$(PtH) = 69 Hz}, respectively. The $CH_2Pt^{IV}$ resonance appears as a singlet with platinum satellites {$^2J$(PtH) = 100 Hz}. The spectrum was well resolved, and all proton resonances were readily assigned (see Experimental Section).

The structure of **3** was determined crystallographically and is shown in Figure 2. Numerous attempts to grow crystals of **3** had been unsuccessful, but crystals were finally obtained by slow diffusion of a mixture of solutions of **2** in acetone with **B** in benzene, the red crystals of **3** forming at the interface. In refinement of the structure by least-squares cycles, the methyl carbon atom C(8) gave an unreasonably small isotropic thermal parameter (0.0089 Å$^2$) and long Pt−C distance (2.25 Å). Of various models used to explain this, the best was to consider a disorder in which the C(8) site was partially occupied by chloride (C:Cl = 0.6:0.4; see Experimental Section for details and other models considered). However, NMR (pure **3** indicated) and EDX analysis (no chloride detected) of crystals from the same sample failed to provide confirmation of the model, which is therefore considered tentative. It may be that the one crystal found suitable for X-ray measurements was atypical of the bulk sample. Otherwise the structure was well defined and clearly confirms the proposed structure of **3**. Selected bond distances and angles are given in Table 1.

There are two octahedral platinum(IV) centers, Pt(1) and Pt(2), with $PtC_3N_2Br$ coordination and one square-planar platinum(II) center with $PtC_2N_2$ (and partly $PtCClN_2$) coordination. Bond distances and angles are

(11) Gould, S.; Strouse, G. F.; Meyer, T. J.; Sullivan, B. P. *Inorg. Chem.* **1991**, *30*, 2942.

(12) Achar, S.; Scott, J. D.; Vittal, J. J.; Puddephatt, R. J. *Organometallics* **1993**, *12*, 4592.

(13) Hasenzahl, S.; Hausen, H.-D.; Kaim, W. *Chem. Eur. J.* **1995**, *1*, 95.

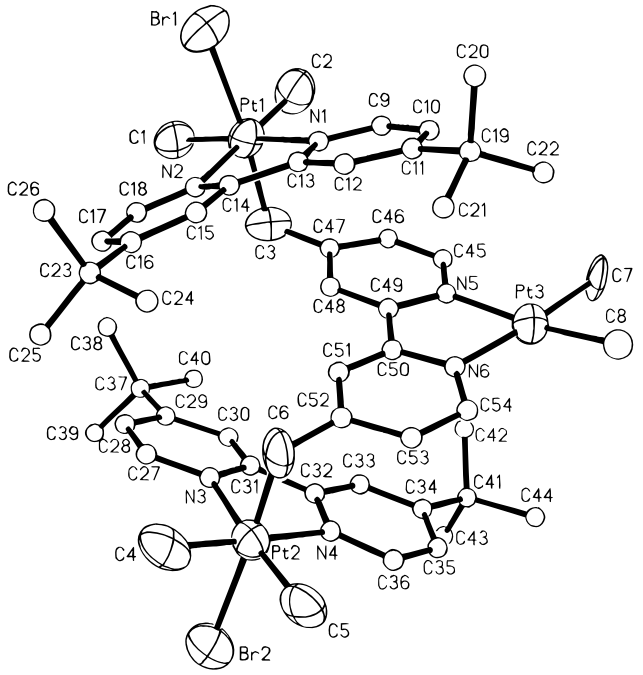


**Figure 2.** A view of the structure of complex **3**. Carbon and nitrogen atoms of pyridine rings and of *tert*-butyl groups are shown as spheres of arbitrary radius. Other heavy atoms (except for C(8)) are shown as 50% probability ellipsoids. The occupancy factor C(8):Cl(1) (not shown) is 0.6:0.4.

**Table 1. Selected Bond Lengths (Å) and Angles (deg)**

| | | | |
|---|---|---|---|
| Pt(1)−C(3) | 2.09(2) | Pt(1)−Br(1) | 2.570(3) |
| Pt(1)−N(1) | 2.16(2) | Pt(1)−N(2) | 2.20(2) |
| Pt(1)−C(1) | 2.07(2) | Pt(1)−C(2) | 2.06(2) |
| Pt(2)−C(6) | 2.05(2) | Pt(2)−Br(2) | 2.553(3) |
| Pt(2)−N(3) | 2.17(2) | Pt(2)−N(4) | 2.18(2) |
| Pt(2)−C(4) | 2.03(2) | Pt(2)−C(5) | 2.05(2) |
| Pt(3)−N(5) | 2.07(2) | Pt(3)−N(6) | 2.11(2) |
| Pt(3)−C(7) | 2.12(2) | Pt(3)−C(8) | 2.12(5) |
| Pt(3)−Cl(1) | 2.32(2) | | |
| C(2)−Pt(1)−C(1) | 86.3(9) | C(2)−Pt(1)−C(3) | 92.4(10) |
| C(1)−Pt(1)−C(3) | 83.7(9) | C(2)−Pt(1)−N(1) | 99.7(8) |
| C(1)−Pt(1)−N(1) | 174.0(8) | C(3)−Pt(1)−N(1) | 96.6(7) |
| C(2)−Pt(1)−N(2) | 174.9(9) | C(1)−Pt(1)−N(2) | 98.2(8) |
| C(3)−Pt(1)−N(2) | 90.6(8) | N(1)−Pt(1)−N(2) | 75.8(6) |
| C(2)−Pt(1)−Br(1) | 90.0(7) | C(1)−Pt(1)−Br(1) | 91.3(7) |
| C(3)−Pt(1)−Br(1) | 174.3(7) | N(1)−Pt(1)−Br(1) | 88.1(4) |
| N(2)−Pt(1)−Br(1) | 87.3(4) | C(4)−Pt(2)−C(5) | 86.6(9) |
| C(4)−Pt(2)−C(6) | 84.9(8) | C(5)−Pt(2)−C(6) | 88.4(9) |
| C(4)−Pt(2)−N(3) | 100.9(8) | C(5)−Pt(2)−N(3) | 172.5(8) |
| C(6)−Pt(2)−N(3) | 93.0(7) | C(4)−Pt(2)−N(4) | 175.6(7) |
| C(5)−Pt(2)−N(4) | 97.4(8) | C(6)−Pt(2)−N(4) | 97.0(7) |
| N(3)−Pt(2)−N(4) | 75.1(6) | C(4)−Pt(2)−Br(2) | 90.5(6) |
| C(5)−Pt(2)−Br(2) | 90.7(7) | C(6)−Pt(2)−Br(2) | 175.3(6) |
| N(3)−Pt(2)−Br(2) | 88.4(4) | N(4)−Pt(2)−Br(2) | 87.7(4) |
| N(5)−Pt(3)−C(8) | 170.7(12) | N(5)−Pt(3)−N(6) | 78.5(6) |
| C(8)−Pt(3)−N(6) | 99.3(13) | N(5)−Pt(3)−C(7) | 97.5(7) |
| C(8)−Pt(3)−C(7) | 84.4(14) | N(6)−Pt(3)−C(7) | 175.6(6) |
| N(5)−Pt(3)−Cl(1) | 173.7(7) | N(6)−Pt(3)−Cl(1) | 96.0(7) |
| C(7)−Pt(3)−Cl(1) | 88.1(7) | | |

consistent with those found in related complexes.[12,14] With respect to the plane of the central $Pt(3)Me_2(bipy)$ fragment, Pt(1) lies above and Pt(2) lies below the plane; this conformation is expected to minimize steric hindrance between the bulky platinum(IV) complex substituents. The solid state conformation allows $\pi$-stacking of the pyridyl rings defined by N(1),C(9)−C(13) and N(5),C(45)−C(49), and by N(4), C(32)−C(36) and N(6),C(50)−C(54).[15] This conformation is not rigid since the $^1$H NMR properties discussed above require a conformation in which there is a plane of symmetry containing the $Pt(3)Me_2(bipy)$ fragment to be easily accessible. This requires easy rotation about the C(3)−C(47) and C(6)−C(52) bonds such that this effective plane of symmetry can contain the C(3)Pt(1) and C(6)Pt(2) bonds and bisect each $Pt^{IV}Me_2$ group.

The formation of **3** represents the end of the first growth cycle in dendrimer formation. The conversion of **1** to **2** leads to doubling of the platinum nuclearity, while conversion of **2** to **3** adds one more platinum atom and regenerates a new $[PtMe_2N_2]$ functionality, which can participate in the next growth cycle. If, after a given growth cycle, the complex contained *n* platinum atoms, the complex obtained in the next growth cycle should contain $2n + 1$ platinum atoms. The expected platinum nuclearities after successive growth cycles would then be 1, 3, 7, 15, 31, etc., with only one of these being a platinum(II) center in each case. Complexes **1** and **3** represent the cases with $n = 1$ and $n = 3$, respectively, and it was of interest to determine how far the sequence could be continued.

**Second Growth Cycle**. In the second growth cycle, trinuclear **3** reacted in a 2:1 molar ratio with **A**, with doubling of the nuclearity to give the pale-yellow hexanuclear platinum(IV) complex **4**, which again contains a free diimine group (Scheme 2). Its UV−visible spectrum showed no peak in the region 340−750 nm (Figure 1), as expected if all platinum(II) centers are consumed, and its $^1$H NMR spectrum shows no peaks due to $BrCH_2$ groups, indicating that these are also completely consumed. The resonances in the $^1$H NMR spectrum of **4** were broader than in **3**, and of course, there are more resonances present. One complication is that, after the oxidative addition to the Pt(3) atom of **3**, there can no longer be a plane of symmetry containing the C(3)Pt(1) and C(6)Pt(2) atoms (nomenclature of Figure 2), and hence doubling of peaks associated with these atoms must occur. The broadening of the peaks is presumed to be due to restricted rotation as the molecule becomes more congested. All the peaks in the $^1$H NMR spectrum could be assigned, but the peak broadening made assignment of $^{195}Pt^1H$ couplings difficult. Details are given in the Experimental Section.

Reaction of the hexanuclear platinum(IV) complex **4** with the dimethylplatinum(II) precursor **B** adds a new platinum(II) center in forming the orange-red heptanuclear complex **5**. The formation of the platinum(II) center could be monitored by appearance of the metal-to-ligand charge transfer band [platinum(II) 5d to $\pi^*$(diimine)] with $\lambda_{max} = 430$ nm, as shown in Figure 1. In the $^1$H NMR spectrum, the $Me_2Pt(II)$ signal appeared at $\delta = 0.65$ and all other resonances remained broad and similar to those in **4**.

Formation of the complex **5** marks the end of the second growth cycle. The reactions in this cycle still occur easily and in very high yield, but the characterization of the products by $^1$H NMR is more challenging

(14) (a) de Felice, V.; Ganis, P.; Vitagliano, A.; Valle, G. *Inorg. Chim. Acta* **1988**, *144*, 57. (b) Annibale, G.; Maresca, L.; Natile, G.; Tiripicchio, A.; Tiripicchio-Camellini, M. *J. Chem. Soc., Dalton Trans.* **1982**, 1587. (c) Albano, V. G.; Braga, D.; de Felice, V.; Panunzi, A.; Vitagliano, A. *Organometallics* **1987**, *6*, 517.

(15) Subramanian, S.; Wang, L. H.; Zaworotko, M. J. *Organometallics* **1993**, *12*, 310.

**Scheme 2**

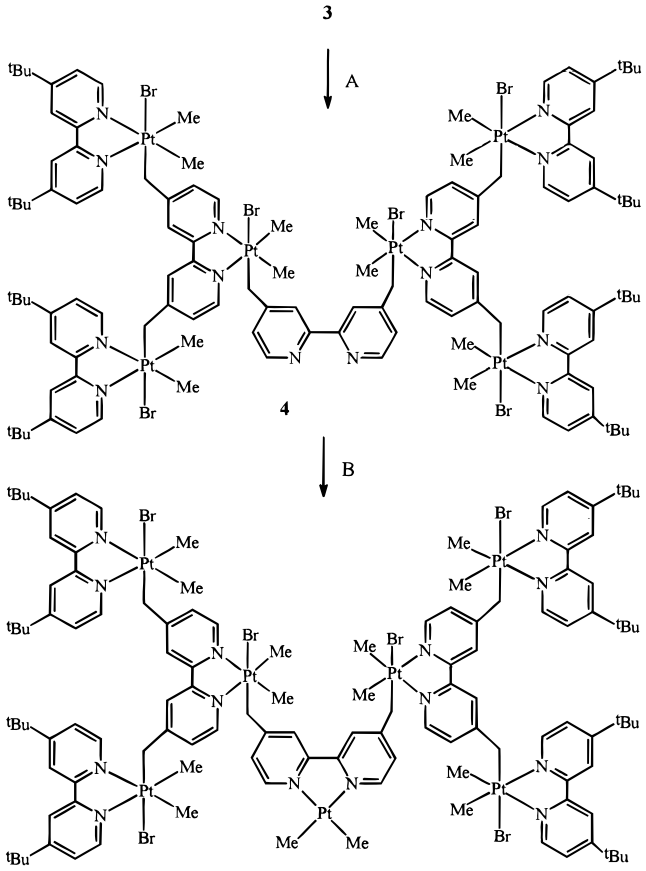


**Scheme 3**[a]

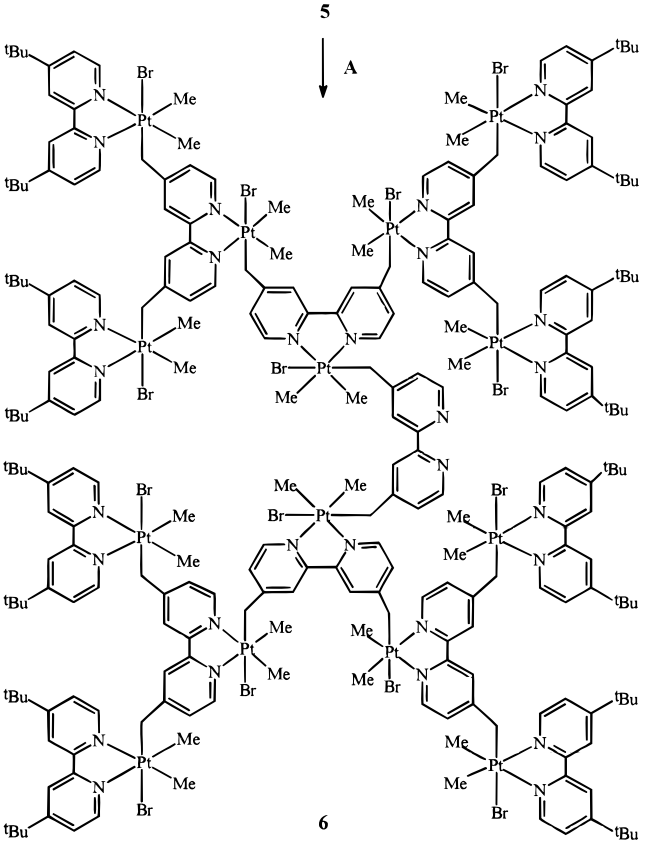


[a] **7** has an extra $PtMe_2$ group bound to the central diimine.

than in the first growth cycle because of extra complexity and signal broadening.

**Third Growth Cycle**. In the third growth cycle, the heptanuclear $Pt^{IV}_6-Pt^{II}$ complex **5** reacted cleanly in a 2:1 molar ratio with **A** to give the pale-yellow $Pt_{14}$ dendrimer **6** (Scheme 3). The evidence for a quantitative reaction is based on the absence of the $CH_2Br$ resonance in the $^1H$ NMR spectrum, which would be present if only partial oxidative addition occurred, and the absence of a MLCT band in the UV−visible, which would be present if some platinum(II) centers remained unreacted. However, the $^1H$ NMR spectra were too broad to allow individual peak assignments and, although integrals of composite bands were consistent with the proposed structure, the characterization of **6** by NMR is not unequivocal. After this stage, the reactions occurred less cleanly. Thus reaction of **6** with the $Me_2Pt$ precursor **B** did not occur quantitatively as judged by the low intensity of the MLCT band for **7**. The impure sample of the $Pt^{IV}_{14}-Pt^{II}$ dendrimer **7** failed to react with more **A** to give a $Pt^{IV}_{30}$ dendrimer. Thus the limit to growth appears to occur after formation of the $Pt_{14}$ dendrimer **6**, with formation of **7** occurring at best in low yield, and further growth not possible. This limit to growth can be understood in terms of steric hindrance. Thus the synthetic method shown in Schemes 1−3 is convergent,[1] with the result that the reaction center becomes more sterically hindered with each growth cycle until a limit is reached at which further reaction is suppressed. In the present case, modification of the reagents to reduce steric hindrance is required to achieve growth beyond the $Pt_{14}$ stage. The solubilities of the complexes follow the sequence **6** ≫ **5**, **4** ≫ **3**, **2** ≪ **1**, as expected since the greater solubility associated with the branched dendrimeric structures is only expected at the second growth cycle.[1] Moreover the increase in the number of the *tert*-butyl groups in the molecule enhances the solubility, and this is also consistent with related observations.[16]

**Larger Organoplatinum Dendrimers.** The above discussion indicates that the synthetic strategy based on oxidative addition and ligand substitution can be successful in the construction of organometallic dendrimers containing up to 14 platinum atoms. Is it possible to prepare higher nuclearity dendrimers by modification of the method? Some progress was made by oxidative addition of the bromomethyl groups of the tetrafunctional reagent 1,2,4,5-tetrakis(bromomethyl)-benzene, **C**, to the platinum(II) center of the complexes **1**, **3**, and **5** (Scheme 4). This method naturally leads to globular architectures with a central benzene core around which the platinum−bipyridyl complexes are arranged in a concentric fashion. In this approach larger fragments are built first (employing convergent method) which are then coupled to a polyfunctional core.

The platinum(II) complexes [$PtMe_2$(2,2′-bipyridine)] and [$PtMe_2$($bu_2$bipy)] reacted in a 4:1 molar ratio with **C** to give the tetranuclear complexes **8** and **9**, respectively (Scheme 4). Complex **8** was insoluble and so it was characterized only by elemental analysis and FAB mass spectroscopy, but **9** was soluble in dichloromethane and was also characterized by NMR. There were two methylplatinum resonances at $\delta = 0.77$, $^2J(PtH) = 68$ Hz, and 0.88, $^2J(PtH) = 68$ Hz, while the $CH_2Pt$

(16) Xu, Z.; Moore, J. S. *Angew. Chem., Int. Ed. Engl.* **1993**, *32*, 246.

**Scheme 4**

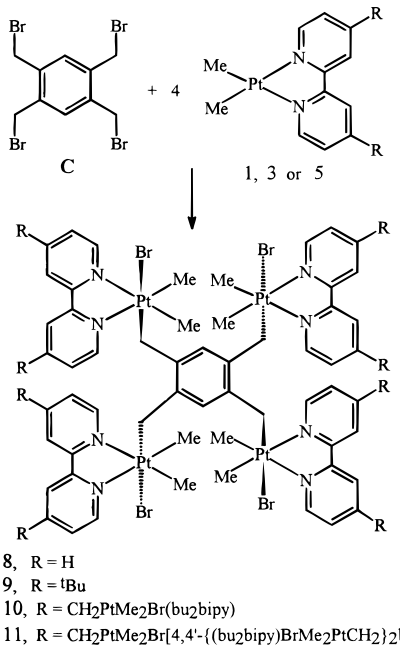


resonance occurred as an AB multiplet, part at $\delta = 2.15$ $\{^2J(\mathrm{PtH}) = 91$ Hz, $^2J(\mathrm{HH})$ ca. 8 Hz$\}$and part obscured by the intense *tert*-butyl resonance at $\delta = 1.5$. Nonequivalence of the $Me_2Pt$ and $CH_2Pt$ protons is expected since there can be no plane of symmetry containing the $BrPtCH_2$ axis, and the magnitudes of the coupling constants $^2J(\mathrm{PtH})$ are characteristic for platinum(IV). A resonance at $\delta = 4.9$ is assigned to the central benzene ring protons ($H^3$, $H^6$), which are strongly shielded by the ring current of the $bu_2$bipy ligands.[7] Steric hindrance in **8** and **9** is expected to be minimized when adjacent platinum(IV) substituents occupy alternating positions above and below the plane of the central benzene ring.

Similarly, the mixed oxidation state complexes **3** and **5** reacted with **C** to yield the dendrimers **10** and **11**, which contain 12 and 28 platinum(IV) centers, respectively. The $Pt_{28}$ complex, containing a total of 1292 atoms, is certainly among the largest transition metal dendrimer yet known.[5,6] The stoichiometry of each reaction was checked by establishing the complete loss of both the MLCT band of the platinum(II) precursor in the UV−visible spectrum and of the $BrCH_2$ resonance in the $^1$H NMR spectrum of the reaction products. The $^1$H NMR spectra of **12** and **13** are broader and individual resonances are not resolved, but peak integrations are still useful and consistent with the proposed structure.

So far, mass spectrometry of the larger dendrimers has failed to yield parent ions, but the molecular sizes could be monitored in a qualitative way by gel permeation chromatography (GPC). The apparent molecular weights by GPC (when referenced to polystyrene standards) were 950, 1300, 1700, 2700, and 3600 for **3**, **9**, **5**, **10**, and **11**, respectively. Naturally, given the standards used, the absolute values are meaningless, but there was a reasonable correlation with the expected molecular weights as shown in Figure 3. This gives further support for the proposed structures.

The melting point onsets as determined by differential scanning calorimetry followed the sequence **8** (270 °C) < **9** (279 °C) < **12** (297 °C) < **13** (312 °C). Similarly,

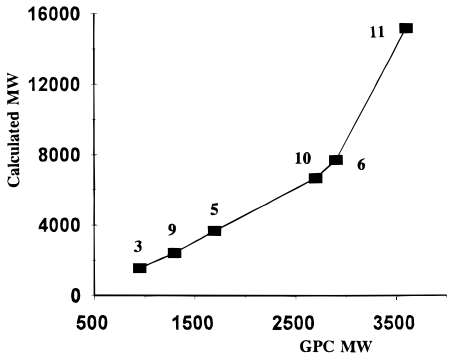


**Figure 3.** Graph of the molecular weights of selected complexes as determined by GPC using polystyrene standards against the calculated molecular weights.

**Scheme 5**

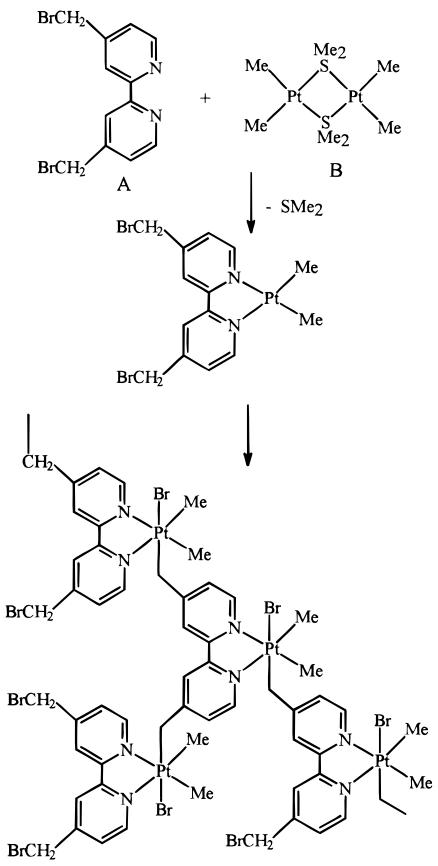


the temperature ranges over which complete decomposition to leave a residue corresponding to the calculated platinum content were, **8** (278−870 °C) < **9** (303−800 °C) < **10** (297−887 °C) < **11** (317−920 °C). It is evident that both the melting points and the decomposition ranges increase with increasing molecular size.

**Synthesis of a Polymeric Organoplatinum Dendrimer.** An uncontrolled dendrimeric growth is observed on the reaction of the dimethylplatinum(II) precursor **B** with 4,4′-bis(bromomethyl)-2,2′-bipyridine, **A**. When solutions of these reagents are mixed, the color rapidly became red, then purple, and finally colorless as an insoluble yellow precipitate formed. The nature of the reactions occurring is not clear since monitoring by NMR failed to identify any of the intermediate complexes, but a tentative interpretation is outlined below (Scheme 5). The first step is believed to be the formation of the red intermediate **12**, which then

reacts immediately by intermolecular oxidative addition of the C−Br bonds to give a purple colored solution which upon continued stirring gives the insoluble yellow polymer, **13**. In the first intermediate there are two $CH_2Br$ groups but only one platinum(II) center, so in the polymer half the $CH_2Br$ groups must remain. It is likely that some of the ligands **A** are doubly platinated, some not at all, and most singly platinated as shown in oversimplified fashion in Scheme 5. It is likely that the growth of the dendrimeric polymer will be limited by steric effects, as in the stepwise oligomerization reactions described above, but insolubility precludes molecular weight determination. This is a form of dendrimer self-assembly.

This work adds significantly to knowledge of dendrimeric bipyridine derivatives as well as their inorganic and organometallic complexes, and the $Pt^{IV}Pt^{II}$ complexes **3** and **5** appear to be the first mixed oxidation state dendrimers.[5,17,18]

## Experimental Section

$^1$H NMR spectra were recorded by using Varian Gemini 200 or XL-300 spectrometers, and mass spectra, by using a Finnigan MAT 8320 spectrometer. Differential scanning calorimetry, DSC, and thermogravimetric analysis (TGA) were carried out by employing Perkin-Elmer DSC7 and TGA7 instruments, respectively. The heating rate was 20 °C/min, and a sample mass of 3−8 mg was used. Nitrogen was used as the purge gas. Gel permeation chromatography was performed using a Waters 600 GPC with Waters 410 differential refractometer as detector. Two ultrastyragel columns were used in series ($10^3$ and $10^2$ Å), and THF was used as the solvent. The system was calibrated with linear polystyrene standards. The UV−visible spectra were recorded using a Cary 2290 spectrophotometer with acetonitrile as solvent. The complexes $[Pt_2Me_4(\mu\text{-}SMe_2)_2]$[8] and $[PtMe_2(bu_2bipy)]$[7] and the diimine 4,4′-bis(bromomethyl)-2,2′-bipyridine[11] were prepared by literature methods. The larger dendrimers reported here are difficult to obtain in analytically pure form, since they do not form well-defined crystals, they occlude solvent and, in some cases, they appear to be hygroscopic by NMR analysis. Fractional precipitation followed by drying and extended pumping under high vacuum gave samples with reasonable analytical purity in most cases (see **6** for details). All reactions were carried out at room temperature.

**Complex 2.** To a stirring red solution of $[PtMe_2(bu_2bipy)]$, **1** (0.10 g), in acetone (10 mL) was added 4,4′-bis(bromomethyl)-2,2′-bipyridine, **A** (0.035 g), in acetone (5 mL). The color of the solution turned yellow, and the product precipitated as a pale yellow solid. It was isolated by filtration and washed thoroughly with ether. Yield: 90%. Anal. Calcd for $C_{52}H_{70}Br_2N_6Pt_2$: C, 47.0; H, 5.3; N, 6.3. Found: C, 47.1; H, 5.3; N, 6.4. FAB MS: *m/z* (%) = 1329 (10%) $[M]^+$, 1269 (100%) $[M - Br]^+$, 1154 (50%) $[M - (2Br + Me)]^+$. $^1$H NMR in $CDCl_3$ (300 MHz): $\delta$ = 1.13 [s, 36H, *t*-Bu]; 1.48 [s, 12H, $^2J$(PtH) = 69 Hz, $Me_2Pt$]; 2.73 [s, 4H, $^2J$(PtH) = 98 Hz, $CH_2Pt$]; 7.28 [dd, 4H, $^3J(H^6H^5)$ = 6 Hz, $^4J(H^3H^5)$ = 1.5 Hz, $H^{5,5'}$ ($bu_2bipy$)]; 7.63 [s, 4H, $H^{3,3'}$ of ($bu_2bipy$)]; 8.48 [d, 4H, $^3J$(PtH) = 18 Hz, $^3J(H^5H^6)$ = 6 Hz, $H^{6,6'}$ of ($bu_2bipy$)]; 6.45 [dd, 2H, $^3J(H^6H^5)$ = 5 Hz, $H^{5,5'}$ of **A**]; 6.64 [s, 2H, $H^{3,3'}$ of **A**]; 7.76 [d, 2H, $^3J(H^5H^6)$ = 5 Hz, $H^{6,6'}$ of **A**]. Melting endotherm onset: 310 °C.

**Complex 3.** To a solution of **2** (0.10 g) in a 1:1 mixture of acetone:benzene (100 mL) was added a solution of $[Pt_2Me_4(\mu\text{-}SMe_2)_2]$ (0.03g) in acetone (5 mL). The solution turned orange-red in color. After 8 h the solvent was evaporated and the product was washed with ether. Yield: 92%. Anal. Calcd for $C_{54}H_{76}Br_2N_6Pt_3$: C, 41.7; H, 4.9; N, 5.4. Found: C, 41.3; H, 5.0; N, 5.05%. $^1$H NMR in $CDCl_3$ (300 MHz): $\delta$ = 0.77 [s, 6H, $^2J$(PtH) = 86 Hz, $Me_2Pt^{II}$]; 1.33 [s, 36H, *t*-Bu]; 1.50 [s, 12H, $^2J$(PtH) = 69 Hz, $Me_2Pt^{IV}$]; 2.80 [s, 4H, $^2J$(PtH) = 100 Hz, $CH_2$-Pt]; 7.45 [d, 4H, $^3J(H^6H^5)$ = 6 Hz, $H^{5,5'}$ ($bu_2bipy$)]; 7.95 [s, 4H, $H^{3,3'}$ of ($bu_2bipy$)]; 8.46 [d, 4H, $^3J$(PtH) = 13 Hz, $^3J(H^5H^6)$ = 6 Hz, $H^{6,6'}$ of ($bu_2bipy$)]; 6.10 [d, 2H, $^3J(H^6H^5)$ = 5 Hz, $^4J$(PtH) = 13 Hz, $H^{5,5'}$ of **A**]; 6.77 [s, 2H, $^4J$(PtH) = 12 Hz, $H^{3,3'}$ of **A**]; 8.22 [d, 2H, $^3J(H^5H^6)$ = 5.5 Hz, $^3J$(PtH) = 21 Hz, $H^{6,6'}$ of **A**]. UV−vis (acetonitrile): $\lambda_{max}$ = 474 nm. Melting endotherm onset: 285 °C.

**Complex 4.** An orange-red solution of **3** (0.10 g) in a 1:1 mixture of acetone:benzene (100 mL) was mixed with a solution of **A** (0.011 g) in acetone (5 mL). The color changed to pale yellow. After 12 h, the solvent was removed and the product was washed with ether and dried under vacuum. Yield: 88%. Anal. Calcd for $C_{120}H_{162}Br_6N_{14}Pt_6$: C, 41.7; H, 4.7; N, 5.7. Found: C, 41.6; H, 5.0; N, 5.8. $^1$H NMR in $CDCl_3$ (300 MHz): $\delta$ = 1.2−1.37 [72H, *t*-Bu], 1.12 and 1.4−1.6 [36H, $Me_2Pt^{IV}$]; 2.1−3.0 [12H, $CH_2Pt(IV)$]; 8.68 and 8.40 [d, 4H each, $H^{6,6'}$ ($bu_2bipy$)]; 8.05 [s, 8H, $H^{3,3'}$ of ($bu_2bipy$)]; 7.28 and 7.58 [d, 4H each, $H^{5,5'}$ of ($bu_2bipy$)]; 5.71 [d, 4H, $H^{5,5'}$ of 1st generation **A**]; 6.83 [s, 4H, $H^{3,3'}$ of 1st generation **A**]; 8.11 [d, 4H, $H^{6,6'}$ of 1st generation **A**]; 6.65 [d, 2H, $H^{6,6'}$ of 2nd generation **A**]; 6.48 [s, 2H, $H^{3,3'}$ of 2nd generation **A**]; note that $H^{5,5'}$ of 2nd generation **A** are obscured. Melting endotherm onset: 306 °C.

**Complex 5.** To a solution of **4** (0.085 g) in acetone (10 mL) was added a solution of **B** (0.015 g) in acetone (5 mL). The solution turned red in color. After 8 h the solvent was removed and the product was washed with ether and dried. Yield: 89%. Anal. Calcd for $C_{122}H_{168}Br_6N_{14}Pt_7$: C, 39.9; H, 4.6; N, 5.8. Found: C, 39.3; H, 4.4; N, 5.4. $^1$H NMR in acetone-$d_6$ (200 MHz): $\delta$ = 0.65 [s, MePt(II)]; 1.1−1.7 [108H, *t*-Bu and MePt-(IV)]; 2.5−3.4 [12H, $CH_2Pt(IV)$]; 6.0−8.9 [42H, bipyridyl]. UV−vis (acetonitrile): $\lambda_{max}$ = 430 nm. Melting endotherm onset: 304 °C.

**Complex 6.** To a solution of **5** (0.065 g) in acetone (10 mL) was added a solution of **A** (0.003 g) in acetone (5 mL). The color changed to pale yellow. After 4 h the solvent was removed and the product was washed with ether and dried. Yield: 75%. It was purified by precipitation from solution in the minimum amount of acetone using ether. Anal. Calcd for $C_{256}H_{346}Br_{14}N_{30}Pt_{14}$: C, 40.0; H, 4.5; N, 5.4. Found: C, 39.3; H, 4.4; N, 5.0. $^1$H NMR in $CDCl_3$ (200 MHz): $\delta$ = 1.0−1.8 [228H, *t*-Bu and $Me_2Pt^{IV}$]; 2.5−3.1 [28H, $CH_2Pt(IV)$]; 6.0−8.8 [m, 90H, aromatic CH].

**Complex 8.** To a stirring solution of $[PtMe_2(bipy)]$ (0.15 g) in acetone (10 mL) was added a solution of 1,2,4,5-tetrakis-

**Table 2. Crystal Data and Experimental Details**[a]

| | |
|---|---|
| formula, fw | $C_{56.6}H_{80.2}N_6Br_2Cl_{0.4}Pt_3 \cdot (CH_3)_2CO$, 1620.53 |
| cryst system, space group | monoclinic, $P2_1/n$ |
| cell dimens | $a$ = 13.131(2) Å<br>$b$ = 19.527(3) Å<br>$c$ = 23.462(3) Å<br>$\beta$ = 90.41(1)° |
| $V$ | 6016(2) Å$^3$ |
| $Z$ | 4 |
| density, calcd (obsd) | 1.79, 1.72(5) g·cm$^{-3}$ |
| temp | 23 °C |
| wavelength, abs coeff | 0.710 73 Å, 8.35 mm$^{-1}$ |
| indepdt reflcns | 7857 [$R$(int) = 0.0643] |
| data/restraints/params | 7853/77/417 |
| goodness-of-fit (GooF) on $F^2$ | 1.018 |
| final $R$ indices [$I > 2\sigma(I)$] | $R1$ = 0.0680, w$R2$ = 0.1361 |
| $R$ indices (all data) | $R1$ = 0.1490, w$R2$ = 0.1761 |

[a] $R1 = \sum(||\boldsymbol{F}_o| - |F_c||)/\sum|F_o|$; w$R2 = [\sum w(F_o^2 - F_c^2)^2/\sum wF_o^4]^{1/2}$; GooF $= [\sum w(F_o^2 - F_c^2)^2/(n - p)]^{1/2}$, where $n$ is the number of reflections and $p$ is the number of parameters refined.

(17) Eisenbach, C. D.; Schubert, U. S.; Baker, G. R.; Newkome, G. R. *J. Chem. Soc., Chem. Commun.* **1995**, 69.

(18) Higashimura, K.; Nakamura, Y. *J. Chem. Soc., Dalton Trans.* **1993**, 3075.

**Table 3. Atomic Coordinates ($\times 10^4$) and Equivalent Isotropic Displacement Parameters ($Å^2 \times 10^3$)**

| atom | *x* | *y* | *z* | *U*(eq)[a] | occu | atom | *x* | *y* | *z* | *U*(eq)[a] | occu |
|---|---|---|---|---|---|---|---|---|---|---|---|
| Pt(1) | 3726.7(7) | 2985.4(5) | 416.7(3) | 62.2(3) | | C(24B) | 8437(21) | 4749(8) | −286(4) | 77(17) | 0.25 |
| Pt(2) | 9404.5(7) | 2037.3(5) | −1495.7(4) | 63.1(3) | | C(25B) | 9055(19) | 3650(11) | 158(14) | 77(17) | 0.25 |
| Pt(3) | 4210.5(8) | 2335.1(4) | −2590.5(4) | 72.3(3) | | C(26B) | 8488(33) | 4625(9) | 781(4) | 77(17) | 0.25 |
| Br(1) | 3337(2) | 4145(2) | 884(1) | 96(1) | | N(3) | 8537(13) | 1697(9) | −765(7) | 65(5) | |
| Br(2) | 10510(2) | 969(2) | −1388(1) | 101(1) | | C(27) | 8777(18) | 1874(11) | −222(10) | 80(7) | |
| C(1) | 3807(17) | 2510(13) | 1207(8) | 82(8) | | C(28) | 8248(18) | 1586(12) | 227(10) | 81(7) | |
| C(2) | 2200(17) | 2746(14) | 423(10) | 92(9) | | C(29) | 7454(16) | 1122(10) | 139(8) | 56(6) | |
| C(3) | 4123(18) | 2019(10) | 111(9) | 69(6) | | C(30) | 7203(15) | 974(10) | −432(8) | 55(6) | |
| C(4) | 10498(17) | 2614(12) | −1108(10) | 82(8) | | C(31) | 7730(16) | 1270(11) | −864(9) | 62(6) | |
| C(5) | 10104(16) | 2274(12) | −2248(10) | 79(7) | | N(4) | 8219(12) | 1379(8) | −1849(7) | 57(5) | |
| C(6) | 8615(15) | 2942(12) | −1558(9) | 72(7) | | C(32) | 7567(15) | 1124(9) | −1467(8) | 53(5) | |
| C(7) | 2680(14) | 2117(13) | −2824(7) | 71(7) | | C(33) | 6756(15) | 708(10) | −1649(8) | 53(5) | |
| C(8) | 4318(35) | 2727(22) | −3430(19) | 35(14) | 0.6 | C(34) | 6572(16) | 581(11) | −2229(9) | 64(6) | |
| Cl(1) | 4534(17) | 2546(11) | −3544(7) | 73(6) | 0.4 | C(35) | 7281(18) | 844(12) | −2597(10) | 79(7) | |
| N(1) | 3807(13) | 3513(8) | −394(7) | 56(5) | | C(36) | 8086(17) | 1231(11) | −2417(9) | 64(6) | |
| C(9) | 3074(18) | 3521(10) | −787(9) | 73(7) | | C(37) | 6919(6) | 776(4) | 646(4) | 86(8) | |
| C(10) | 3211(16) | 3863(10) | −1303(9) | 61(6) | | C(38) | 6559(9) | 1318(5) | 1078(7) | 99(9) | |
| C(11) | 4078(16) | 4235(11) | −1409(9) | 60(6) | | C(39) | 7678(8) | 286(6) | 940(8) | 138(13) | |
| C(12) | 4780(18) | 4205(12) | −989(10) | 74(7) | | C(40) | 5994(9) | 366(7) | 425(7) | 125(12) | |
| C(13) | 4676(15) | 3840(10) | −491(8) | 52(5) | | C(41) | 5682(5) | 137(4) | −2420(3) | 92(8) | |
| N(2) | 5321(14) | 3322(9) | 363(7) | 66(5) | | C(42) | 4721(7) | 384(8) | −2107(6) | 108(7) | 0.75 |
| C(14) | 5505(16) | 3777(10) | −83(8) | 57(6) | | C(43) | 5916(16) | −609(5) | −2248(8) | 108(7) | 0.75 |
| C(15) | 6469(16) | 4063(11) | −122(9) | 64(6) | | C(44) | 5499(16) | 175(12) | −3069(3) | 108(7) | 0.75 |
| C(16) | 7235(17) | 3900(11) | 257(9) | 66(6) | | C(42A) | 5954(15) | −39(10) | −3041(4) | 95(21) | 0.25 |
| C(17) | 7004(20) | 3439(12) | 687(10) | 82(7) | | C(43A) | 4709(19) | 579(18) | −2413(10) | 95(21) | 0.25 |
| C(18) | 6048(18) | 3185(11) | 722(10) | 71(7) | | C(44A) | 5497(34) | −529(8) | −2084(10) | 95(21) | 0.25 |
| C(19) | 4207(3) | 4653(2) | −1981(3) | 75(7) | | N(5) | 4088(13) | 2117(8) | −1731(7) | 58(5) | |
| C(20) | 3770(8) | 5377(3) | −1890(11) | 74(10) | 0.4 | C(45) | 3255(17) | 1873(9) | −1445(9) | 67(6) | |
| C(21) | 5362(4) | 4702(7) | −2088(11) | 74(10) | 0.4 | C(46) | 3236(18) | 1806(11) | −867(10) | 75(7) | |
| C(22) | 3682(13) | 4319(13) | −2501(9) | 74(10) | 0.4 | C(47) | 4066(16) | 2006(11) | −525(9) | 62(6) | |
| C(20A) | 4158(10) | 5415(3) | −1814(10) | 81(15) | 0.4 | C(48) | 4950(15) | 2223(10) | −826(8) | 55(6) | |
| C(21A) | 5212(5) | 4511(10) | −2295(8) | 81(15) | 0.4 | C(49) | 4939(16) | 2275(11) | −1410(9) | 61(6) | |
| C(22A) | 3301(7) | 4478(11) | −2376(8) | 81(15) | 0.4 | N(6) | 5695(12) | 2564(8) | −2294(7) | 58(5) | |
| C(20B) | 4347(11) | 5379(5) | −1735(11) | 70(26) | 0.2 | C(50) | 5835(15) | 2529(9) | −1732(8) | 50(5) | |
| C(21B) | 5234(7) | 4391(14) | −2209(17) | 70(26) | 0.2 | C(51) | 6722(16) | 2680(10) | −1501(9) | 61(6) | |
| C(22B) | 3420(23) | 4673(14) | −2471(12) | 70(26) | 0.2 | C(52) | 7582(17) | 2871(11) | −1810(9) | 66(6) | |
| C(23) | 8295(4) | 4247(3) | 214(2) | 78(7) | | C(53) | 7427(17) | 2895(11) | −2412(9) | 66(6) | |
| C(24) | 8484(14) | 4427(8) | −416(2) | 73(8) | 0.5 | C(54) | 6463(17) | 2730(11) | −2638(10) | 68(6) | |
| C(25) | 9159(8) | 3782(8) | 435(8) | 73(8) | 0.5 | O(1)[b] | 2562(6) | 646(12) | 640(8) | 161(9) | |
| C(26) | 8267(19) | 4910(5) | 570(6) | 73(8) | 0.5 | C(55)[b] | 1686(6) | 681(12) | 778(4) | 122(11) | |
| C(26A) | 8042(12) | 5010(3) | 306(6) | 89(19) | 0.25 | C(56)[b] | 1363(24) | 678(18) | 1408(6) | 156(14) | |
| C(25A) | 9023(12) | 4001(8) | 689(5) | 89(19) | 0.25 | C(57)[b] | 788(17) | 727(19) | 353(12) | 200(19) | |
| C(24A) | 8808(14) | 4155(9) | −370(4) | 89(19) | 0.25 | | | | | | |

[a] *U*(eq) is one-third of the trace of the orthogonalized $\mathbf{U}_{ij}$ tensor. [b] Solvent.



(bromomethyl)benzene (0.045 g) in acetone (5 mL). The solution color changed from orange red to yellow. After the solution was stirred for 4 h, the solvent was removed and the product was washed with ether. Yield: 80%. Anal. Calcd for $C_{58}H_{66}Br_4N_8Pt_4$: C, 35.3; H, 3.4; N, 5.7. Found: C, 35.0; H, 3.0; N, 6.0. FAB MS: *m*/*z* (%) = 1894 (10%) $[M - HBr]^+$. Melting endotherm onset: 270 °C. Similarly the following were prepared.

**Complex 9.** Anal. Calcd For $C_{90}H_{130}Br_4N_8Pt_4$: C, 44.6; H, 5.4; N, 4.6. Found: C, 43.8; H, 5.7; N, 4.3. $^1$H NMR in $CD_2Cl_2$ (300 MHz): $\delta$ = 0.65 [s, 12H, $^2J$(PtH) = 68 Hz, $Me_2Pt$]; 0.88 [s, 12H, $^2J$(PtH) = 68 Hz, $Me_2Pt$]; 1.45 [s, 72H, *t*-Bu]; 2.1 [m, 4H, $^2J$(PtH) = 91 Hz, $CH_2Pt$, see text]; 7.52 [d, 8H, $H^{5,5'}$ ($bu_2bipy$)]; 8.20 [s, 8H, $H^{3,3'}$ of ($bu_2bipy$)]; 8.26 [d, 8H, $H^{6,6'}$ of ($bu_2bipy$)]; 4.9 [s, 2H, benzene ring protons].

**Complex 10.** Anal. Calcd for $C_{226}H_{314}Br_{12}N_{24}Pt_{12}$: C, 40.7; H, 4.7; N, 5.0. Found: C, 39.8; H, 4.6; N, 4.7. $^1$H NMR in $CDCl_3$ (200 MHz): $\delta$ = 1.0−1.8 [br, 216H, *t*-Bu and MePt]; 2.6−3.2 [br, 24H, $CH_2Pt$]; 5.8−8.8 [br, 74H, aromatic H].

**Complex 11.** Anal. Calcd for $C_{498}H_{682}Br_{28}N_{56}Pt_{28}$: C, 39.5; H, 4.5; N, 5.2. Found: C, 38.8; H, 4.3; N, 5.0. $^1$H NMR in $CDCl_3$ (200 MHz): $\delta$ = 1.1−1.7 [br, 456H, *t*-Bu and MePt]; 2.5−3.2 [br, 56H, $CH_2Pt$]; 5.9−9.0 [br, 170H, aromatic H].

**Polymer 13**. To a solution of $[Pt_2Me_4(\mu\text{-}SMe_2)_2]$ (0.075g) in acetone (10 mL) was added a solution of 4,4′-bis(bromomethyl)-2,2′-bipyridine (0.90 g) in acetone (5 mL). The solution turned red instantly, then purple, and finally very pale yellow. The precipitated solid was separated and washed with ether. Yield: 95%. Anal. Calcd for $(C_{14}H_{16}Br_2N_2Pt)_n$: C, 29.6; H, 2.8; N, 4.9. Found: C, 29.7; H, 2.8; N, 5.4.

**X-ray Structure Determination of 3.** Orange-red, platy crystals were grown from acetone/benzene (see text). A crystal of size 0.28 × 0.17 × 0.08 mm was mounted on a glass fiber for the diffraction experiments. The density measurements were made by the neutral buoyancy method. The diffraction experiments were carried out using a Siemens P4 diffractometer with the XSCANS software package[19] and using graphite-monochromated Mo Kα radiation at 23 °C. The cell constants were obtained by centering 25 high-angle reflections ($24.6 \leq 2\theta \leq 25.0°$). The Laue symmetry 2/*m* was determined by merging symmetry equivalent reflections. A total of 9731 reflections were collected in the $\theta$ range 1.8−22.5° ($-1 \leq h \leq 14$, $-1 \leq k \leq 21$, $-25 \leq l \leq 25$) using the $\theta$−$2\theta$ scan mode at variable scan speeds (2−10 deg/min). Background measurements were made at the ends of the scan range. Three standard reflections were monitored at the end of every 297 reflections. An empirical absorption correction was applied to the data ($\mu$ = 8.35 $mm^{-1}$). The space group $P2_1/n$ was determined from the systematic absences ($h0l$, $h + l = 2n + 1$ and $0k0$, $k = 2n + 1$). The data processing, solution, and the initial refinements were carried out using the SHELXTL-PC programs.[20] The final refinements were performed using the SHELXL-93 software programs.[21] The methyl carbon atoms present in three *tert*-butyl groups were found to be disordered.

(19) XSCANS, Siemens Analytical X-Ray Instruments Inc., Madison, WI, 1990.

The disorder models were constructed from the difference Fourier routines. Three orientations were found for the methyl carbon atoms bonded to C(19) (occupancy ratios 0.4:0.4:0.2) and C(23) (occupancy ratios 0.5:0.25:0.25) and two orientations for the methyl carbon atoms bonded to C(41) (occupancy ratio 0.75:0.25) and were included in the least-squares refinements. Common isotropic thermal parameters were refined for each set of methyl carbon atoms. These disordered *tert*-butyl groups were treated as idealized tetrahedrons (with C−C distance 1.542 Å and C−C−C angle 109.5°). No hydrogen atoms were included for these disordered groups.

During the least-squares cycles, an unreasonably small isotropic thermal parameter (0.0089 Å) and long Pt−C distance (2.25 Å) were observed for the C(8) carbon atom attached to Pt(II). In the difference Fourier map, the number of electrons in the C(8) site was deduced to be 10.8 by comparing with that in the site C(7). This indicated that the C(8) site may also be occupied by an atom heavier than carbon that forms a bond longer than the Pt−C bond. On the basis of this, a fraction of chlorine atom was assumed to be occupying the C(8) site also. This disorder model was included in the final least-squares cycles with the occupancy of C(8) and Cl(1) in the ratio 0.6:0.4. The thermal parameters, bond distances, and residual electron densities could be accounted for satisfactorily using this model. In another attempt, carbon and Br atoms were included (in the ratio 0.85:0.15) in the refinements but the Pt−Br distance was too short (2.309 Å) to be reasonable, and hence, this model was discarded. Further, the unresolved oval-shaped contours obtained in the electron density maps support the presence of Cl rather than Br. All the Pt, Br, Cl, and methyl carbon atoms were refined anisotropically. In the final least-squares refinement cycles on $F^2$, the model converged at $R_1 = 0.0680$, w$R_2 = 0.1361$, and Goof = 1.018 for 4139 observations with $F_o \geq 4\sigma(F_o)$ and 417 parameters, and $R_1 = 0.1490$, w$R_2 = 0.1761$ for all 7853 data. In the final difference Fourier synthesis the electron density fluctuated in the range 0.88 to −0.74 e Å$^{-3}$; of the top five peaks three were near Pt atoms (1.07−1.30 Å), one near C(26A), and one near Cl(1) at a distance of 0.85 Å. The mean and the maximum shift/esd in the final cycles were 0.002 and 0.23, respectively. The experimental details and crystal data and the positional and thermal parameters are in Tables 2 and 3. Complete bond distances and angles, anisotropic thermal parameters, hydrogen atom coordinates, and selected weighted least-squares planes have been included in the Supporting Information.

**Acknowledgment.** We thank the NSERC (Canada) for financial support and Dr. N. C. Payne for valuable advice.

**Supporting Information Available:** Tables of bond distances and angles, anisotropic thermal parameters, hydrogen atom coordinates and *U* values, selected torsion angles, and selected weighted least-squares planes and an ORTEP diagram (9 pages). Ordering information is given on any current masthead page.

OM950413M

(20) Sheldrick, G. M. SHELXTL-PC Software, Siemens Analytical X-Ray Instruments Inc., Madison, WI, 1990.
(21) Sheldrick, G. M. SHELXL-93, University of Gottingen, 1993.